Development of Autonomous Underwater Vehicle towards Visual Servo Control

Chanop Silpa-Anan[†] **Samer Abdallah**[†] and **David Wettergreen**[‡*]

Robotic Systems Laboratory
[†]Department of Engineering, FEIT
[‡]Department of Systems Engineering
Australian National University, Canberra, ACT 0200, Australia
http://wwwsyseng.anu.edu.au/rsl/

Abstract

We are developing a visually-guided autonomous underwater vehicle. We have implemented a computed torque controller, using Euler parameters, for position and velocity control. This formulation eliminates singularity in the model and controller and offers some degrees of coupling between vehicle degrees of freedom. A calibrated thruster model which computes thrust output from measured voltage and current, provides input to the thrust controller . We are now adding the vision into the system for visually-servoed guidance.

Figure 1: Kambara solid model.

1 Introduction

At the Australian National University, we are developing an autonomous underwater vehicle (AUV), named Kambara [Wettergreen *et al.*, 1999]. Major objectives are to enable Kambara to autonomously follow along fixed natural and artificial features, and swim after dynamic targets. These abilities would help Kambara to perform underwater inspection tasks, such as exploring the sea floor and studying marine creatures.

Kambara is equipped with an on-board computing unit, various kind of sensors, a pan-tilt camera, and a stereo vision system. We are using the stereo vision system for tracking targets, and extracting target position, velocity and orientation. We have developed area-based feature tracking for following features from frame to frame.

We are developing a computed torque controller for controlling a vehicle position and velocity. Since an AUV is usually highly coupled between multiple degrees of freedom, by using computed torque control, we will have some degrees of coupling between vehicle degrees of freedom. In general, the performance of the computed torque controller depends on accuracy of system

model. We developed Kambara model based on model proposed in [Fossen and Fjellstad, 1994] which use Euler parameters as an attitude representation to eliminate singularity in the system. We also developed a thruster model and thruster controller which use estimated thrust from measured voltage and current, in order to control force and torque required by the vehicle computed torque controller.

By combining the vision system and vehicle controller, Kambara can track targets and move relative to them autonomously. Thus Kambara can operate in a mission like following a reef, following a pipe, or chasing a fish.

This paper starts by describing the Kambara model in section 2, followed by the vehicle controller in section 3. The thuster model and controller are proposed in section 4 and 5. Section 6 shows the result of using the Kambara model and vehicle controller in a simulation study. A visual servo guidance for target tracking is proposed in section 7.

2 Kambara Modeling

We have developed a mathematical modeling for Kambara based on [Fossen and Fjellstad, 1994]. In this model, we use Euler parameters for attitude representation instead of conventional Euler angles. The benefit

---

of using Euler parameters over Euler angles is that the singularity that occurs in system dynamic equations is eliminated.

Define a position state vector $\mathcal{P} = [\mathbf{x}^\top, q^\top]^\top$, where $\mathbf{x} = [x, y, z]^\top$, and $\mathbf{q} = [\eta, \epsilon^\top]^\top$, $\epsilon = [\epsilon_1, \epsilon_2, \epsilon_3]^\top$. Here $\mathbf{x}$ and $\mathbf{q}$ are the position vector and Euler parameters representing Kambara attitude in the world-fixed reference frame $\{W\}$.

Define a velocity state vector $\mathcal{V} = [\mathbf{v}^\top, \omega^\top]^\top$, where $\mathbf{v} = [u, v, w]^\top$ and $\omega = [p, q, r]^\top$. Here $\mathbf{v}$ and ω are the linear and angular velocity vectors in the Kambara reference frame $\{K\}$.

Define a torque/force input vector $\mathcal{T} = [\mathcal{T}_1^\top, \mathcal{T}_2^\top]^\top$, where $\mathcal{T}_1 = [X, Y, Z]^\top$ and $\mathcal{T}_2 = [K, M, N]^\top$. Here $\mathcal{T}_1$ and $\mathcal{T}_2$ are force and torque vectors in the Kambara reference frame $\{K\}$.

The general system dynamics of Kambara in the $\{K\}$ frame can be written as

$$M\dot{\mathcal{V}} + C(\mathcal{V})\mathcal{V} + D(\mathcal{V})\mathcal{V} + g(\mathbf{q}) = \mathcal{T}, \qquad (1)$$

where M is a mass/inertia matrix, including hydrodynamic added mass/inertia, C is a Coriolis and centripetal matrix, including hydrodynamic added Coriolis and centripetal mass/inertia, D is a hydrodynamic damping matrix, and g is a gravity and buoyancy force vector.

Define $M = M_{RB} + M_A$, where M_{RB} is a rigid body mass/inertia matrix, and M_A is a hydrodynamic added mass/inertia matrix given by

$$M_{RB} = \begin{bmatrix} mI_{3\times3} & -mS(r_G) \\ mS(r_G) & I_k \end{bmatrix};$$

$$M_A = -\begin{bmatrix} X_{\dot{u}} & X_{\dot{v}} & X_{\dot{w}} & X_{\dot{p}} & X_{\dot{q}} & X_{\dot{r}} \\ Y_{\dot{u}} & Y_{\dot{v}} & Y_{\dot{w}} & Y_{\dot{p}} & Y_{\dot{q}} & Y_{\dot{r}} \\ Z_{\dot{u}} & Z_{\dot{v}} & Z_{\dot{w}} & Z_{\dot{p}} & Z_{\dot{q}} & Z_{\dot{r}} \\ K_{\dot{u}} & K_{\dot{v}} & K_{\dot{w}} & K_{\dot{p}} & K_{\dot{q}} & K_{\dot{r}} \\ M_{\dot{u}} & M_{\dot{v}} & M_{\dot{w}} & M_{\dot{p}} & M_{\dot{q}} & M_{\dot{r}} \\ N_{\dot{u}} & N_{\dot{v}} & N_{\dot{w}} & N_{\dot{p}} & N_{\dot{q}} & N_{\dot{r}} \end{bmatrix}.$$

In the above, m is the Kambara mass, I_k is the inertia matrix, r_G is center of gravity and $S(\lambda)$ is a skew-symmetric matrix operator of vector λ given by

$$S(\lambda) = \begin{bmatrix} 0 & -\lambda_3 & \lambda_2 \\ \lambda_3 & 0 & -\lambda_1 \\ -\lambda_2 & \lambda_1 & 0 \end{bmatrix}, \ S(\lambda) = -S^\top(\lambda).$$

SANAME notation is used here, for instance the hydrodynamic added mass force Y_A along y axis which due to acceleration $\dot{u}$ in x direction is written as

$$Y_A = Y_{\dot{u}}\dot{u} \text{ , where } Y_{\dot{u}} = \frac{\partial Y}{\partial \dot{u}}$$

To simplify the matrix M, we locate the origin of the Kambara reference frame $\{K\}$ at the center of gravity so

that $r_G = [0, 0, 0]^\top$. Since Kambara is almost symmetric in all planes, M_{RB} can be approximated as

$$M_{RB} = diag\{m, m, m, I_{xx}, I_{yy}, I_{zz}\}.$$

We simplify M_A so that it contains only diagonal values.

$$M_A = diag\{X_{\dot{u}}, Y_{\dot{v}}, Z_{\dot{w}}, K_{\dot{p}}, M_{\dot{q}}, N_{\dot{r}}\}.$$

Define $C = C_{RB} + C_A$, where C_{RB} is the rigid body Coriolis and centripetal matrix, and C_A is the hydrodynamic added Coriolis and centripetal matrix.

Let

$$M_A = \begin{bmatrix} A_{11} & A_{12} \\ A_{21} & A_{22} \end{bmatrix}.$$

C_{RB} and C_A are

$$C_{RB} = \begin{bmatrix} 0_{3\times3} & -mS(\mathbf{v}) \\ -mS(\mathbf{v}) & -S(I\omega) \end{bmatrix};$$

$$C_A = \begin{bmatrix} 0_{3\times3} & -S(A_{11}\mathbf{v} + A_{12}\omega) \\ -S(A_{11}\mathbf{v} + A_{12}\omega) & -S(A_{21}\mathbf{v} + A_{22}\omega) \end{bmatrix}.$$

Usually D is a complicated function of $\mathcal{V}$, but we use a rough approximation of D as:

$$
\begin{aligned}
D = \ & -diag\{X_u, Y_v, Z_w, K_p, M_q, N_r\} \\
& -diag\{X_{u|u|}|u|, Y_{v|v|}|v|, Z_{w|w|}|w|, \\
& K_{p|p|}|P|, M_{q|q|}|q|, N_{r|r|}|r|\}.
\end{aligned}
$$

A Jacobean matrix $J(\mathbf{q})$ is used to relate the position state vector $\mathcal{P}$ and velocity state vector $\mathcal{V}$.

$$
\begin{aligned}
\dot{\mathcal{P}} &= J(\mathbf{q})\mathcal{V} \\
\begin{bmatrix} \dot{\mathbf{x}} \\ \dot{\mathbf{q}} \end{bmatrix} &= \begin{bmatrix} R(\mathbf{q}) & 0 \\ 0 & \frac{1}{2}U(\mathbf{q}) \end{bmatrix} \begin{bmatrix} \mathbf{v} \\ \omega \end{bmatrix},
\end{aligned}
$$

where

$$R(\mathbf{q}) = \begin{bmatrix} 1 - 2\epsilon_2^2 - 2\epsilon_3^2 & 2(\epsilon_1\epsilon_2 - \eta\epsilon_3) & 2(\epsilon_1\epsilon_3 + \eta\epsilon_2) \\ 2(\epsilon_1\epsilon_2 + \eta\epsilon_3) & 1 - 2\epsilon_1^2 - 2\epsilon_2^2 & 2(\epsilon_2\epsilon_3 - \eta\epsilon_1) \\ 2(\epsilon_1\epsilon_3 - \eta\epsilon_2) & 2(\epsilon_2\epsilon_3 + \eta\epsilon_1) & 1 - 2\epsilon_1^2\epsilon_2^2 \end{bmatrix}$$

and

$$U(\mathbf{q}) = \begin{bmatrix} -\epsilon^\top \\ \eta I_{3\times3} + S(\epsilon) \end{bmatrix}.$$

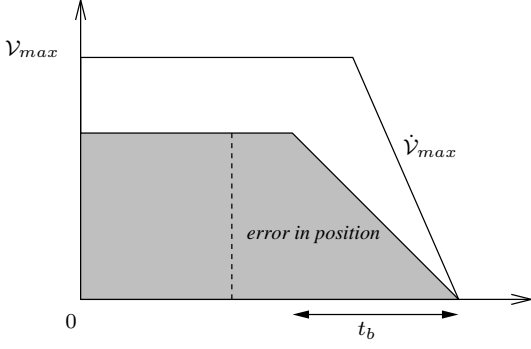Thus with this model we can compute Kambara's position and velocity from applied forces and torques.

Figure 2: Velocity profile used for determining $\mathcal{V}_d$ and $\dot{\mathcal{V}}_d$ from position error.

3 Vehicle Controller

There have been several approaches proposed for controlling the position and velocity of AUVs, these include traditional PID control, adaptive control, sliding control, and learning control [Wettergreen et al., 1999]. In many AUVs , PID control is commonly used because of its simplicity. Usually, vehicle controller is implement in multiple single degree of freedom (DOF) controllers, having one stand alone controller for each DOF. Since an AUV is usually highly coupled between multiple DOFs due to vehicle hydrodynamic and thruster configuration, performance of controller can be improved by using controller that couples between multiple DOFs.

Kambara is an open frame AUV (see Figure 1). It has two main water tight enclosures for the computing unit, sensors, the pan-tilt camera and the battery. Five thrusters are rigidly attached to the Kambara frame. These five thrusters provide Kambara 5 DOFs in surge, heave, roll, pitch and yaw, but not direct sway. However, Kambara can roll to a certain degree and move side-ways while keeping the altitude constant to get an effect of sway. For Kambara to move along in one DOF without affecting other DOFs with the current thruster configuration, it can not fire just one single thruster. A combination of two, three, or all five thrusters is needed to create a movement in one direction. Thus Kambara is highly coupled between DOFs by thruster configuration as well as due to hydrodynamic coupling.

We opted to develop a computed torque controller, since it offers some degrees of the coupling between multiple DOFs through computed torque component. From the system dynamics equation (1), computed torque control law can be written as

$$\mathcal{T} = \alpha \mathcal{T}' + \beta,$$

where $\alpha = M$, and $\beta = C(\mathcal{V})\mathcal{V} + D(\mathcal{V})\mathcal{V} + g(\mathbf{q})$. Here β cancels the nonlinear and the coupling components and $\mathcal{T}'$ implements the linear control law.

We choose a PID control tracking controller for $\mathcal{T}'$ as:

$$\mathcal{T}' = \dot{\mathcal{V}}_d + k_v \dot{\varepsilon} + k_{vi} \int \dot{\varepsilon} + k_p \varepsilon + k_{pi} \int \varepsilon,$$

where $\dot{\varepsilon} = \mathcal{V}_d - \mathcal{V}$ and $\varepsilon = {}^K\mathcal{P}_d - {}^KP$. Here ${}^KP$ is vector P in the $\{K\}$ frame.

The Euler parameter component of $\mathcal{P}$ is not a direct subtraction but $\mathbf{q}_e = \mathbf{q}^{-1}\mathbf{q}_d$ where a multiplication of two $\mathbf{q}$s is

$$\mathbf{q}_1\mathbf{q}_2 = \left[\begin{array}{cc} \eta_1 & -\epsilon_1^\top \\ -\epsilon_1^\top & \eta_1 I_{3\times3} + S(\epsilon_1) \end{array} \right] \left[\begin{array}{c} \eta_2 \\ \epsilon_2 \end{array} \right]$$

and an inverse of $\mathbf{q}$ is

$$\mathbf{q}^{-1} = \left[\begin{array}{c} \eta \\ -\epsilon \end{array} \right].$$

.

Since we have an approximate model, β will not cancel out all the non-linearity and coupling in the system. The terms $k_{vi}\int \dot{\varepsilon}$ and $k_{pi}\int \varepsilon$ are involved for minimizing error during tracking.

Let $\mathcal{U} = [T_1, T_2, T_3, T_4, T_5]^\top$ be a vector of thrusts from five thrusters (horizontal left, horizontal right, vertical left, vertical right and vertical rear). Define a matrix L a 6×5 mapping matrix such that

$$\mathcal{T} = L\mathcal{U}.$$

We can find a 5×6 matrix $\tilde{L}$ that satisfies

$$\mathcal{U} = \tilde{\mathcal{L}}\mathcal{T}.$$

Since Kambara has 5 DOFs and 5 thrusters, the force for sway motion in $\mathcal{T}$ is not mapped back to $\mathcal{U}$.

The computed torque controller that we have designed is a tracking controller which needs ${}^KP_d$, $\mathcal{V}_d$ and $\dot{\mathcal{V}}_d$ as reference input. Traditionally ${}^KP_d$, $\mathcal{V}_d$ and $\dot{\mathcal{V}}_d$ are calculated from trajectory planning. But recalculating the trajectory every time the target position changes could be computationally expensive or have some other difficulties in implementation. Instead of doing full trajectory planning, we use the right hand side of a trapezoidal velocity profile, see Figure 2, for calculating $\mathcal{V}_d$ and $\dot{\mathcal{V}}_d$. The velocities $\mathcal{V}_d$ and $\dot{\mathcal{V}}_d$ are calculated from the position error vector, ε . There are two parameters in designing this trapezoidal velocity profile, $\mathcal{V}_{max}$ and $\dot{\mathcal{V}}_{max}$. The value of $\mathcal{V}_{max}$ could be obtained from Kambara's physical maximum velocity, while $\dot{\mathcal{V}}_{max}$ could be obtained from its physical maximum acceleration. The trapezoidal velocity profile should be within the $\mathcal{V}_{max}$, $\dot{\mathcal{V}}_{max}$ velocity profile.
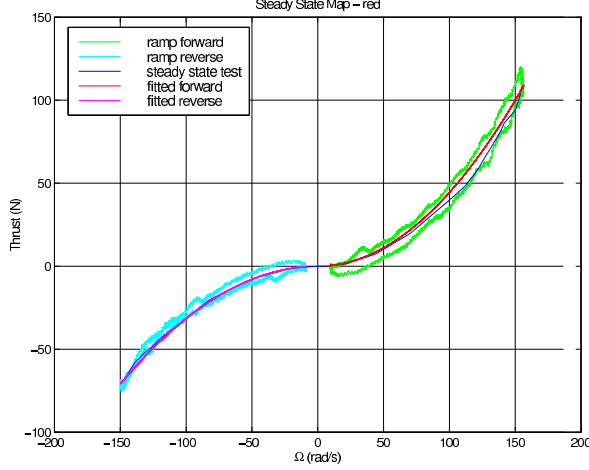
Figure 3: Calibration of thruster using steady state thrust model and estimated shaft velocity. $T = k\Omega|\Omega|$ where $k = 4.19 \times 10^{-3} \frac{N}{rad^2/sec^2}$ for forward thrust, and $k = 3.12 \times 10^{-3} \frac{N}{rad^2/sec^2}$ for reverse thrust.

4   Thruster Modeling

The five thrusters installed in Kambara are modified electric trolling motors with cut down propellers and added ducts. With these modifications, the original thruster specifications, if they were publically available would be useless. Calibration is needed in order to be able to control thrust.

One of the simplest ways to control thrust is to use steady state thrust to represent all the behavior of the thruster. It is well known, [Whitcomb and Yoerger, 1999], that under bollard-pull conditions, steady state thrust can be modeled as

$$T = \rho A R^2 \eta^2 \tan^2(p)\Omega|\Omega|, \qquad (2)$$

Where T is the thrust output, ρ is fluid density, A is the duct/propeller area, R is the propeller radius, η is the propeller efficiency, p is the propeller pitch angle, and Ω is the shaft velocity.

In [Bachmayer *et al.*, 2000], Whitcomb proposed a complex thruster model which requires an accurate measurement of several motor/thruster parameters, as well as the online measurement of the shaft velocity, Ω.

Several proposed thruster model suggest that in order to control the thrust, T, the propeller angular velocity, Ω, must be controlled according to thruster model.

Because of thruster configuration and limited available space inside the nose of the thruster, we decided to put neither a shaft encoder nor a tachometer to measure shaft velocity. Thus, we need to develop an alternative way to estimate shaft velocity in order to control thrust output.
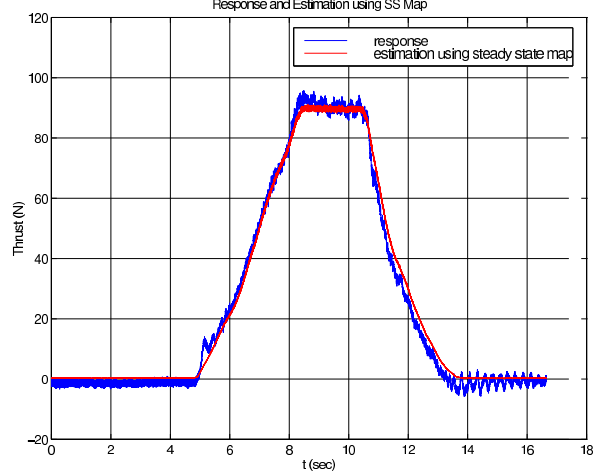

Figure 4: Plot of estimated thrust output, using steady state model and estimated Ω, versus thrust measurement for ramp input.

We proposed to use the motor electro-dynamics to estimate shaft velocity. The thruster that we are using is a permanent magnet DC motor. The general dynamic equations for a permanent magnet DC motor are

$$e = iR_w + L_w\frac{di}{dt} + k_{emf}\Omega \qquad (3)$$

$$k_t i = J\dot{\Omega} + friction + \tau_{load} \qquad (4)$$

Where e is the motor voltage, i is the motor current, Ω is the shaft velocity, R_w is the winding resistance, L_w is the winding inductance, k_{emf} is the motor back emf constant, k_t is the motor torque constant, J is the motor inertia, $friction$ is the motor friction, and τ_{load} is the motor load

Friction is modeled as

$$friction(\Omega) = k_{f0}sign(\Omega) + k_{f1}\Omega \qquad (5)$$

where $k_{f0}sign(\Omega)$ is the coulomb friction, and $k_{f1}\Omega$ is the viscous friction.

For many DC motor control applications, L_w is usually low and may be neglected since time constant induced by L_w is negligible compare to the motor time constant. Rearranging equation 3 gives

$$\Omega = \frac{e - iR_w}{k_{emf}}. \qquad (6)$$

We calibrated the thrusters by simultaneously measuring thrust output, command voltage and current drained by thruster. Figure 3 shows that our calibration result, using estimates of Ω, is in agreement with steady state model $T = k\Omega|\Omega|$. In Figure 4, we evaluated steady state model with ramp transient response. The result
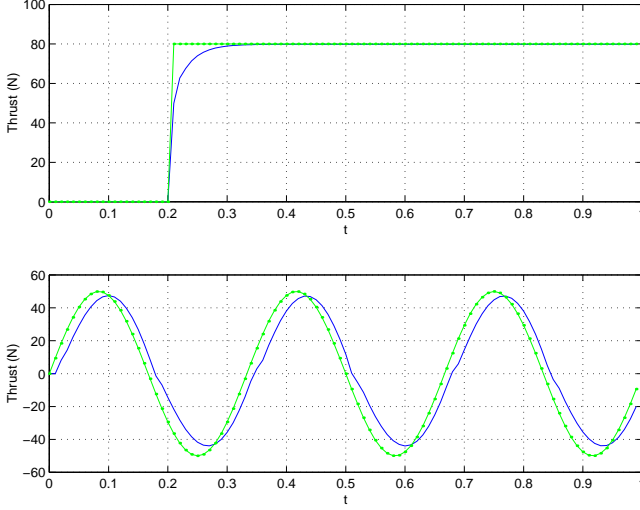
Figure 5: Simulation result of nonlinear PI thruster controller, $K_P = 0.1$, $K_i = 10$, step response and sine wave response, $f = 5\,Hz$.

shows that steady state model $T = k\Omega|\Omega|$ can be used for thrust estimation. We observed some degree of fluctuations in thrust at the start of transient response that this model could not accurately reproduce.

5 Thruster Controller

In our system, we use pulse width modulation (PWM) amplifiers to drive the thrusters. These PWM amplifiers are voltage amplifiers which have current sensors sending signals back to the controller. The PWM signal generator and thruster controller will be implemented on a Motorola 68332 CPU.

We have designed a nonlinear PI controller for controlling the thruster. In using PI control in the motor/amplifier application, there is usually an "integrator windup" phenomenon. Such phenomenon could degrade the controller performance with lag response and/or overshoot. We are implementing saturation integrator to overcome this problem.

For the thruster controller, K_p and K_i are currently hand tuned. Saturation level of the integrator is limited to the maximum voltage output of PWM amplifier. Fine tuning of K_p and K_i will be determined empirically on the real system.

From simulation, we found that using higher K_p and K_i will result in faster response, but the motor will also drain higher current. The level of current drawn from the motor is another aspect in tuning the controller since over current may degrade the magnet in the motor and can possibly damage the amplifier.

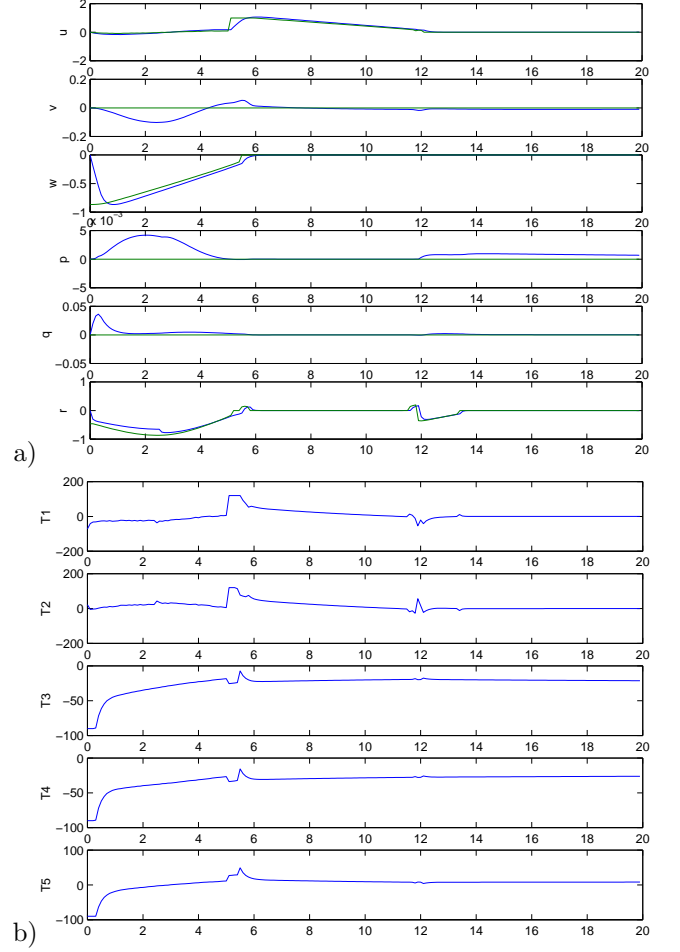Figure 5 shows step and sine wave responses of the nonlinear PI controller. The system exhibits a lag re-

Figure 6: Simulation results. a) Velocity $\mathcal{V}$, solid line and $\mathcal{V}_d$, dot line; b) Thruster command $\mathcal{U}$.

sponse under a sine wave input. The response could be made faster by tuning controller with higher K_p and K_i gains.

6 Simulation Study

We use the Kambara model and computed torque controller developed in the section 2 and 3 to do a simulation study. Figures 6 and 7 show simulation results of moving the vehicle from initial position $[0, 0, 0]^\top$, heading $0\,rad$, to target position $[-5, -1.5, -3]^\top$, heading $\pi\,rad$. During simulation study, we found that using the computed torque controller alone gives a satisfactory result when $\triangle\mathcal{P}$ is small. Since Kambara cannot do direct swaying, for large $\triangle\mathcal{P}$, Kambara position might not converge to desired target position. This is where the trajectory planner has an important role. In this example, a simple trajectory planner which use only surge and yaw motions in x-y plane is used. From the example, Kambara is orienting itself to the target position, during the first 6 seconds, before moving forward, but it is allowed to move
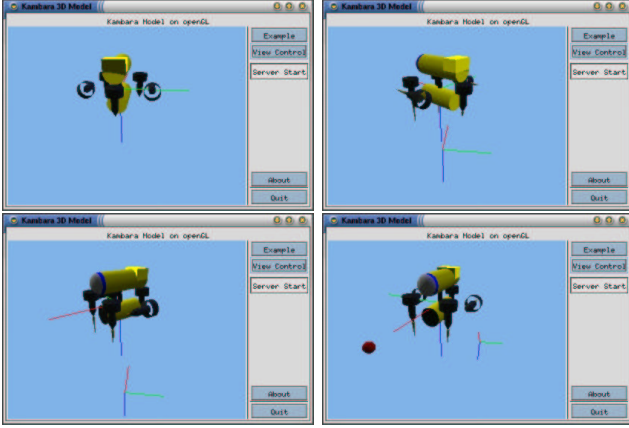
Figure 7: Simulation of Kambara with initial position $[0, 0, 0]^{\top}$, initial heading $0\,rad$, target position $[-5, -1.5 - 3]^{\top}$, target heading $\pi\,rad$.

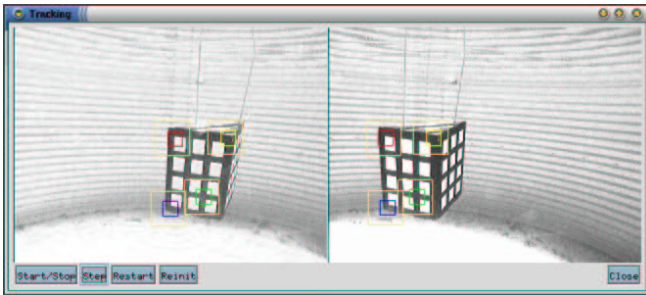Figure 8: Multiple features ZNCC tracking of a calibration target in stereo images.

freely in the z direction, since there is no constraint in the z-axis.

An intelligent trajectory planning scheme can be optimized to enable Kambara to move to the target within minimum time or using minimum power.

7 Visual Servo Control

We have developed a stereo area-based feature matching function for tracking the target. The stereo system will output the position of a feature relative to Kambara. With the current hardware, we are using a look and move visual servo method for tracking the target.

For the task of tracking the moving target, the position and velocity of the features/target are extracted from visual information. Then, the position and velocity of the target are used to calculate the desired vehicle position and velocity such that it would track/follow moving target.

For the task of keeping stationary with respect to the fixed target, we are tracking multiple features of one target, e.g. 4 features for a planar target. Then, the target orientation, and position relative to Kambara can be ex-

tracted from visual information. Such information could then be use as the desired position and orientation references which are used to drive Kambara.

In both cases, we use fast area-based methods for tracking features. An optimized zero mean normalized cross correlation (ZNCC) technique has been developed. In figure 8, we use ZNCC to track multiple features in stereo images. In this initial implementation, the single template without template updating is being used. We found that if feature being tracked change appearance due to relative motion between the camera and target, the tracking target is quickly lost. Multiple templates and template updating schemes are under development in order to provide more robustness.

8 Conclusions

This paper proposes an approach for visually-guiding an AUV. We have developed the Kambara mathematical model and computed torque controller in a simulation study. With a good mathematical model, computed torque control gives a satisfactory results in controlling vehicle position and velocity. The thruster model which estimates the thrust from motor voltage and current has been developed and verified in field test. The implementation of vehicle controller and thruster controller on Kambara is in progress, with testing to follow.

The vision system which is another key part for visually-guiding the AUV is in early development. A robust 3D tracking technique for underwater vision is underway.

References

[Bachmayer et al., 2000] Ralph Bachmayer, Louis L. Whitcomb, and M. A. Grosenbaugh. An accurate four-quadrant nonlinear dynamical model for marine thruster: Theory & experimental validation. *IEEE Journal of Oceanic Engineering*, 25(1), January 2000.

[Fossen and Fjellstad, 1994] Thor I. Fossen and Ola-Erik Fjellstad. Position and attitude tracking of auvs: A quaternion feedback approach. *IEEE Journal of Ocenic Engineering*, 19(4):512–518, October 1994.

[Wettergreen et al., 1999] David Wettergreen, Chris Gaskett, and Alex Zelinsky. Autonomous guidance and control for an underwater robotic vehicle. In *Proceedings of the International Conference on Field and Service Robotics (FSR'99)*, Pittsburgh, USA, September 1999.

[Whitcomb and Yoerger, 1999] Louis L. Whitcomb and Dana R. Yoerger. Development, comparison, and preliminary experimental validation of non-linear dynamic thruster models. *IEEE Journal of Oceanic Engineering*, 24(4):481–494, October 1999.